Interfacial N Vacancies in GaN/(Al,Ga)N/GaN Heterostructures

Vera Prozheeva,[1] Ilja Makkonen,[2] Haoran Li,[3] Stacia Keller,[3] Umesh K. Mishra,[3] and Filip Tuomisto[1,2,*]

[1] *Department of Applied Physics, Aalto University, P.O. Box 15100, FI-00076 Aalto, Finland*

[2] *Department of Physics and Helsinki Institute of Physics, University of Helsinki, P.O. Box 43, FI-00014 Helsinki, Finland*

[3] *Electrical and Computer Engineering Department, University of California, Santa Barbara, California, USA*

(Received 16 October 2019; revised manuscript received 7 January 2020; accepted 24 March 2020; published 13 April 2020)

We show that N-polar GaN/(Al, Ga)N/GaN heterostructures exhibit significant N deficiency at the bottom (Al, Ga)N/GaN interface, and that these N vacancies are responsible for the trapping of holes observed in unoptimized N-polar GaN/(Al, Ga)N/GaN high electron mobility transistors. We arrive at this conclusion by performing positron annihilation experiments on GaN/(Al, Ga)N/GaN heterostructures of both N and Ga polarity, as well as state-of-the-art theoretical calculations of the positron states and positron-electron annihilation signals. We suggest that the occurrence of high interfacial N vacancy concentrations is a universal property of nitride semiconductor heterostructures at net negative polarization interfaces.

DOI: 10.1103/PhysRevApplied.13.044034

I. INTRODUCTION

Originally developed as special components for a supercomputer, HEMTs eventually proceeded to volume production and were successfully integrated in a multitude of every-day-use devices [1]. HEMTs based on III nitrides grant higher 2DEG densities due to polarization fields intrinsic to the wurtzite structure when compared to Si-containing or GaAs/(Al, Ga)As heterostructures [2–4]. The direction of polarization, Ga or N polarity, strongly influences the sheet-carrier density of the 2DEG. Traditionally, the study of GaN was devoted to Ga-polar (0001) direction only. Recently, N-polar heterostructures have gained interest thanks to their advantages for high-frequency and high-power transistors. N-polar GaN-based devices with record output power densities well beyond Ga-polar devices have been demonstrated [5]. They offer a substantial reduction in energy consumption of power-distribution systems in cell phones, computers, radiolocators, and industrial equipment as compared to GaAs-based devices [1].

N-polar HEMTs with unoptimized barrier design and doping suffer from large-signal dispersion and are sensitive to light, issues attributed to the presence of donorlike hole traps close to the valence band within the device structure [3,6–8]. These defects are identified to be located at the bottom (Al, Ga)N/GaN interface of N-polar HEMTs. The negative impact of the traps can be mitigated by an appropriate design combined with Si doping, where the Fermi level is kept away from the valence band and the trap level [3]. Unevenly distributed gap states have also been observed in Ga-polar (Al, Ga)N/GaN HEMTs [9]. Nevertheless, the origin of the interface traps in N-polar (Al, Ga)N HEMTs has remained unknown.

In this work, we show that the bottom (Al, Ga)N/GaN interface of N-polar GaN/(Al, Ga)N/GaN heterostructures contains nitrogen vacancies V_N at high concentrations. Nitrogen vacancies are deep donors in both GaN and AlN [10,11], indicating that they are likely to be the origin of the excess positive charge at this interface, which can impact the performance of the devices if not accounted for in the design of the epitaxial layer structure. We arrive at these conclusions by performing positron annihilation spectroscopy [12] on both N- and Ga-polar heterostructures grown by metal-organic chemical vapor deposition (MOCVD). Earlier theoretical calculations have shown that positrons act as interface-sensitive probes in polar semiconductor heterostructures [13].

II. METHODS

A schematic cross section of a typical N-polar HEMT is presented in Fig. 1(a). The epitaxial structures studied in this work are schematically presented in Figs. 1(c)–(e), including three N-polar HEMT-like structures with graded composition of Al from 5 to 38% in (Al, Ga)N:Si layer and varying Si doping (c), constant composition (ungraded) Ga- and N-polar samples with $Al_{0.25}Ga_{0.75}N$ (d), and Ga- and N-polar multi-quantum-well (MQW) samples with four periods of $Al_{0.4}Ga_{0.6}N$/GaN (e). All samples

*filip.tuomisto@helsinki.fi

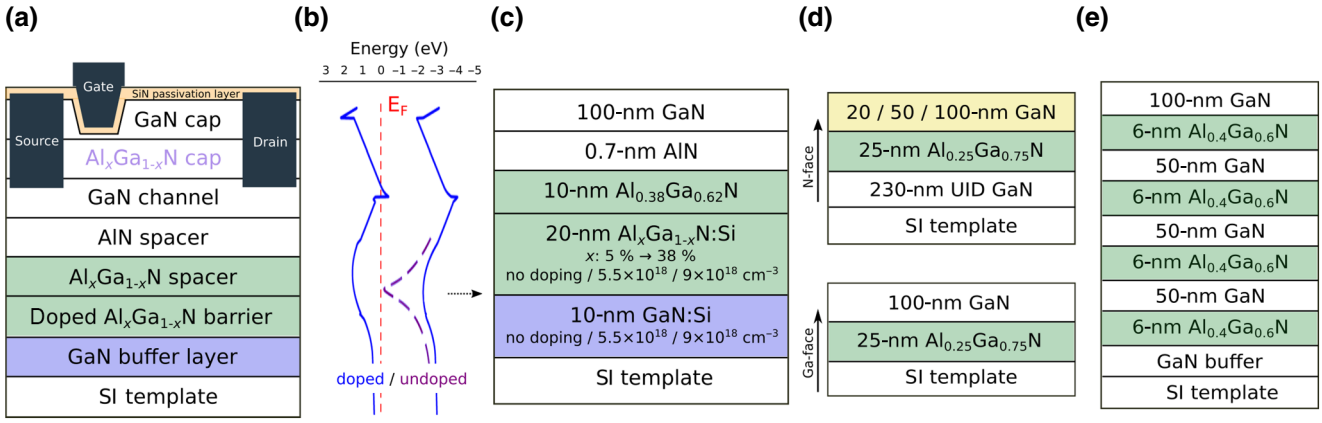

FIG. 1. (a) Schematic cross section of a typical N-polar HEMT. (b) Schematic energy band diagram of N-polar undoped and highly doped GaN/(Al, Ga)N/GaN heterostructures (after Ref. [3]). (c) Schematic of the undoped and Si-doped GaN/(Al, Ga)N/GaN N-polar heterostructure with graded (Al, Ga)N layer, [Si] $= 5.5 \times 10^{18}$ cm^{-3}/9×10^{18} cm^{-3}. (d) Schematics of constant composition (ungraded) N- and Ga-polar heterostructures. (e) Schematic structure of Ga-/N-polar MQW samples.

are composed of about 1.5-μm-thick semi-insulating (SI) GaN base layers, followed by the (Al, Ga)N barrier layers and the GaN channel, which is positioned on top of the (Al, Ga)N barrier in the N-polar direction. Substrates with a misorientation of 4° from the *a*-sapphire plane are used for the N-polar samples—the crystal misorientation was previously identified as one of the key components for a robust N-polar growth process enabling the deposition of high-quality and high-purity N-polar (Al,Ga)N films [14]. Details of the growth conditions are reported in Refs. [15,16].

Figure 1(b) shows a schematic energy band diagram for the N-polar GaN/(Al, Ga)N/GaN heterostructures in this work, adapted from Ref. [3]. In the undoped structure, the valence band is touching the Fermi level leading to electron-hole recombination at the bottom (Al, Ga)N/GaN interface, while in the structure with high Si doping ([Si] $= 9 \times 10^{18}$ cm^{-3}), the valence band is significantly lower than the Fermi level, thus preventing the modulation of donor traps. The macroscopic electric fields drives the positrons to the same interface as holes in the undoped structure, causing spatial confinement of the positron state at that interface [13].

We perform both conventional and coincidence Doppler broadening measurements of positron annihilation radiation with a variable-energy positron beam using high-purity germanium (HPGe) detectors with an energy resolution of 1.2 keV at 511 keV. The integration windows for the *S* and *W* parameters describing the shape of the Doppler broadened 511-keV annihilation line are set to $|p_L| < 0.4$ a.u. and 1.6 a.u. $< |p_L| < 4.0$ a.u., respectively. Operating two HPGe detectors in coincidence mode enables accurate study of the momenta of the core electrons, providing the identification of the chemical surroundings of the annihilation site. For details of the technique and data analysis, see Ref. [12].

We use *ab initio* electronic structure calculations to model the positron states and annihilation parameters in N vacancy-containing GaN/AlN superlattice structures using 256-atom (0001) wurtzite supercell, which is a $2 \times 2 \times 1$ repetition of the cell used in Ref. [13]. The valence electron densities are obtained self-consistently via the local-density approximation (LDA), employing the projector augmented-wave (PAW) method [17], and the plane-wave code VASP [18–20]. The positron states and annihilation characteristics are determined using the LDA [21] and the state-dependent scheme [22] for the momentum densities of annihilating electron-positron pairs [23,24]. For comparison with experiments, the computed Doppler spectra are convoluted with the energy resolution of the experimental setup.

III. RESULTS AND DISCUSSION

Conventional Doppler broadening results for N-polar heterostructures with graded Al composition (c) are presented in Fig. 2. High *S* parameter at low implantation energies 0–3 keV results from positron annihilations at the surface states. At an implantation depth of 50–250 nm, positrons probe the (Al, Ga)N/GaN layers. It is important to note that the implantation profile widens with the implantation energy, and the extent of the profile is roughly twice the mean implantation depth [26]. The implantation energy range 4–14 keV is thus characteristic of the bottom (Al, Ga)N/GaN interface. There the effect of Si doping immediately manifests itself in an increase (decrease) of the *S* (*W*) parameter compared to the undoped sample. There is no observable difference between the two doping levels, 5.5×10^{18} cm^{-3} and 9×10^{18} cm^{-3}. Plotting the *S* and *W* parameters with implantation energy as the running parameter (see Fig. 3) from the surface to about 20 keV results in a straight line, for both the undoped and

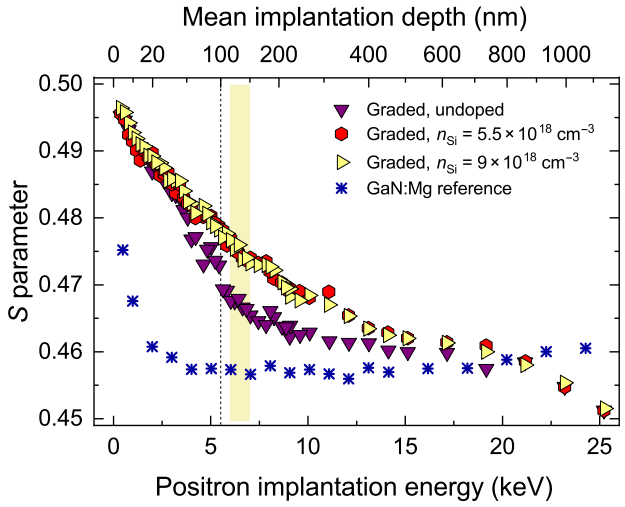

FIG. 2. S parameter as a function of positron implantation energy and mean implantation depth in graded design GaN/(Al, Ga)N/GaN heterostructures. The region of maximal difference between the undoped and doped structures is highlighted. The GaN reference parameters are obtained from high-quality GaN:Mg where positrons only annihilate in the free state in the lattice [25].

the doped samples, as the lattice state, surface state, and Ga vacancy state are almost aligned as is typical of GaN [27–30]. Hence the only conclusion that can be drawn from the (S, W) plot in Fig. 3 is that the 100-nm N-polar GaN cap on top of the (Al, Ga)N barrier contains a fairly high concentration of Ga vacancy-related defects.

To get a better insight into the changes in the S and W parameters, the positron data are analysed by fitting the stationary positron diffusion equation using the VEPFIT program [31]. Both the S and W parameters and the positron diffusion length are fitted simultaneously employing a three-layer model for N-polar heterostructures. Due to the complexity of the layer models, the absolute values

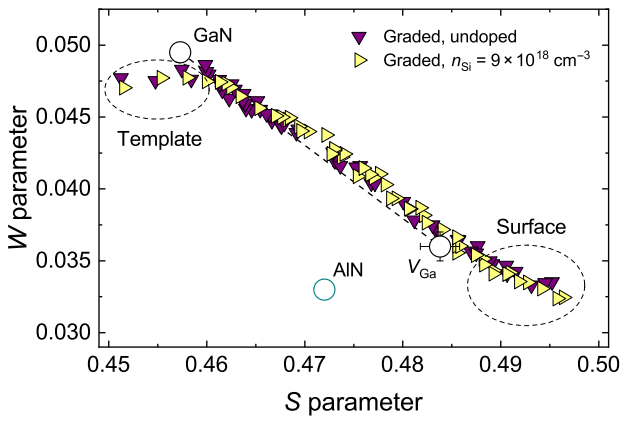

FIG. 3. (S, W) parameters for undoped and Si-doped GaN/(Al, Ga)N/GaN heterostructures.

of positron diffusion lengths obtained with the fits should be treated as indicative, and only the relative changes are used as a basis for interpretation.

The fitted effective positron diffusion length L_{eff}^{+} in N-polar heterostructures with graded Al content doubles (from 15 ± 5 nm to 35 ± 5 nm) for the (Al, Ga)N layer and grows over tenfold (from 5 ± 5 nm to 80 ± 15 nm) for the bottom GaN layer when Si doping is introduced. Importantly, an increase in the effective diffusion length indicates a reduction in the positron trapping rate at defects [12]. The low L_{eff}^{+} around the bottom interface in the undoped heterostructure leads to the abrupt decrease of the S parameter at a mean implantation depth of 100 nm (6–7-keV implantation energy) highlighted in Fig. 2. The backdiffusion of positrons in the doped samples induces much more gradual reduction of the S parameter. Typically, a higher S parameter indicates more positrons getting trapped at vacancy defects such as the Ga vacancy V_{Ga} in GaN [32–34], or positrons getting trapped at bigger vacancy defects. However, the increase in the S parameter is in this case associated with the increase of the effective positron diffusion length. Note that Si doping in (Al, Ga)N and GaN is known to slightly increase or not affect at all the cation vacancy concentration, but not a strong decrease that would cause significant changes in the effective positron diffusion length [25,32,35]. This implies substantial positron trapping at the bottom (Al, Ga)N/GaN interface of the undoped heterostructure, with an interface-trap characteristic S parameter that is lower than that of the V_{Ga}-type defects.

The positron sensitivity to the defect states at the bottom (Al, Ga)N/GaN interface is further supported by the results obtained in the heterostructures with varying GaN-cap thickness and constant composition $Al_{0.25}Ga_{0.75}N$ layer (d). Remarkably, the S parameter of the heterostructure with undoped $Al_xGa_{1-x}N$ layer with graded Al content (c) is indistinguishable from that of the heterostructure with constant composition as shown in Fig. 4. The top panel of Fig. 4 shows that the effect of the reduced effective positron diffusion length is most pronounced for the structure with a 100-nm-thick GaN cap, and hence is the choice of the cap thickness for the heterostructures.

The design of the epitaxial structure of the MQW samples (e) is such that it maximizes the positron annihilation signal originating from the interface of interest, as suggested by the results in Figs. 2 and 4. Figure 4 shows that the positron annihilation signal from the N-polar MQW is similar to the undoped heterostructure with graded Al content at depths below the GaN cap (shaded region). At higher energies $E > 20$ keV the data for the N-polar MQW structure do not converge towards the S parameter of the GaN template due to the higher thickness of the structure. There is a clear difference between the N- and Ga-polar samples: the positrons are insensitive to the possible defects present at the bottom interface of each

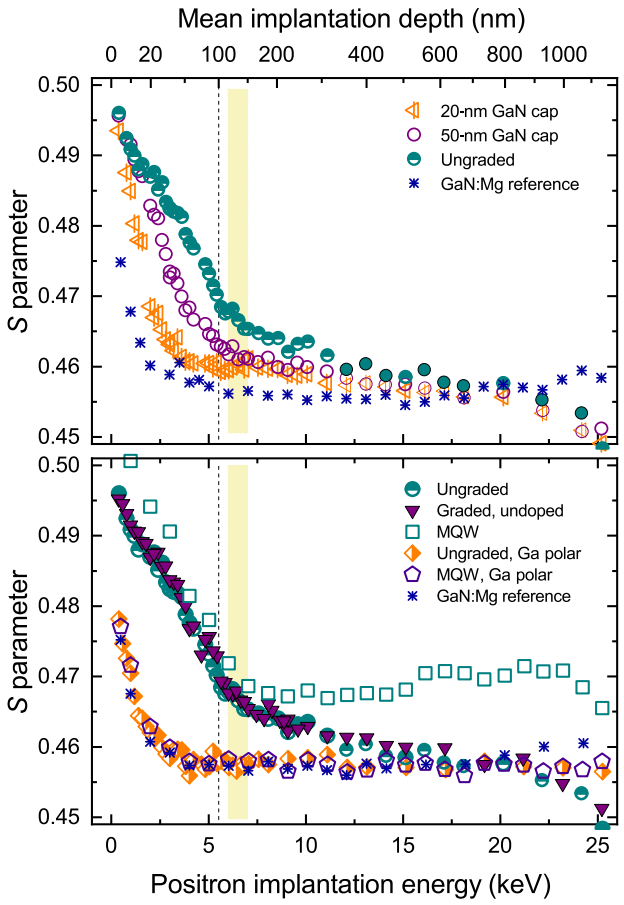

FIG. 4. *S* parameter as a function of positron implantation energy and mean implantation depth in constant composition (ungraded) design heterostructures and MQWs (bottom panel). The structures are N polar unless Ga polarity is indicated. GaN-cap-thickness optimization. The most pronounced signal is obtained from the sample with the 100-nm GaN cap referred to as "ungraded" (top panel).

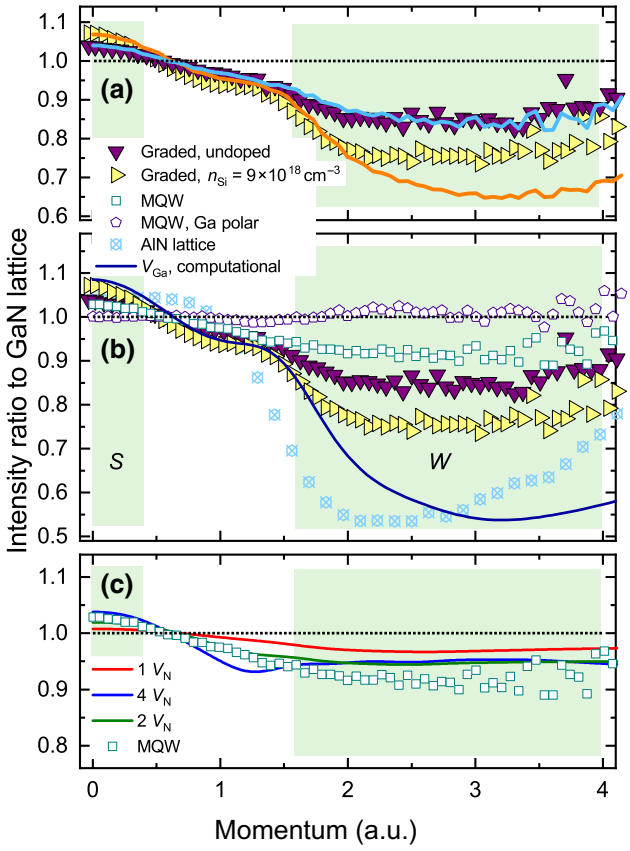

FIG. 5. (a) Normalized coincidence Doppler spectra (ratio curves) and linear combinations of N-polar MQW signal and V_{Ga} for the undoped and doped samples. (b) Ratio curves of the studied heterostructures measured at room temperature. The structures are N polar unless Ga polarity is indicated. (c) Ratio curves of the N-polar MQW sample and calculated V_N for a different number of N vacancies at the AlN/GaN interface in the supercell. The calculated curve for the AlN/GaN structure with no vacancies (not shown) is indistinguishable from the structure with 1 V_N. Regions representative of the (*S*, *W*) parameters are highlighted.

(Al, Ga)N layer in the Ga-polar samples as the positrons are attracted to the top interface.

We further investigate the nature of the defect state at the bottom (Al, Ga)N/GaN interface by performing Doppler measurements in coincidence mode. The ratio curves obtained at 7-keV implantation energy (shaded region in Fig. 2) for the heterostructures with graded Al content (c) and N- and Ga-polar MQWs (e) are presented in Fig. 5(b), normalized to the GaN reference. The ratio curves for the AlN lattice and for the theoretically calculated V_{Ga} (theory and experiment coincide for V_{Ga} [36,37]) are shown for comparison.

Clearly, the measured data do not contain any AlN lattice-related signal as expected for a structure constrained to the in-plane GaN lattice constant [13]. The ratio curve for the Ga-polar MQW is close to 1 confirming that Ga-polar structures from a positron point of view are similar to the GaN lattice as seen in Fig. 4. At low momenta $p_L < 0.6$ a.u., all coincidence Doppler spectra for the N-polar structures have higher intensity compared to the GaN reference, indicating positron annihilation at open-volume defects. At higher momenta, the signal intensities for the N-polar samples decrease, also indicative of open-volume defects. However, the ratio curve for the N-polar MQW neither has the shoulderlike feature of V_{Ga} at $1 < p_L < 1.5$ a.u. nor can it be modeled as a linear combination of unity and V_{Ga}-like signal, see Fig. 5(a). This means that the data obtained in the N-polar MQW structure, representative of the bottom (Al, Ga)N/GaN interface, indicate the presence of open-volume defects at the interface but this open volume is not related to V_{Ga}.

The shape of the ratio curve of the undoped heterostructure with graded Al content (c) strongly resembles that of the N-polar MQW (e) interface characteristic and can be

represented as a linear combination of about 80% interface and 20% V_{Ga} signals [top curve in Fig. 5(a)]. The V_{Ga} component can be explained by the broad positron implantation profile, where part of the signal originates from the GaN cap. The Si-doped heterostructure with graded (Al, Ga)N layer is clearly different: the closest match is obtained with 25%–30% of interface and 70%–75% of V_{Ga}, yet it does not fully describe the shoulder feature at $p_L < 1.5$ a.u. and has lower intensity in the high momentum region [bottom curve in Fig. 5(a)]. The weak contribution of the interface signal to the coincidence data for the doped heterostructure compared to that for the undoped structure confirms strong electric-field-driven positron trapping at the bottom (Al, Ga)N/GaN interface and is in excellent agreement with energy-band-diagram modeling [3] and predictions for positron confinement in polar heterostructures [13].

The small fraction of V_{Ga} observed in the coincidence data for the undoped heterostructure with Al gradient and no V_{Ga}-related component in the interface signal [see MQW in Fig. 5(b)] suggest that nitrogen vacancies V_N could be the key to a detailed understanding of the positron annihilation data. Importantly, the MQW interface signal is different from that calculated for the perfect AlN/GaN interface [13], and in the case of (Al, Ga)N/GaN interface it should in fact rather closely resemble the GaN lattice signal due to the lower fraction of Al in the system. Figure 5(c) shows ratio curves for the MQW sample, representative of the bottom (Al, Ga)N/GaN interface, and theoretically calculated AlN/GaN heterostuctures containing different amounts of N vacancies V_N at the interface. It is important to note that N vacancies placed elsewhere in the supercell, irrespective of whether simple GaN or AlN, or an interface structure is considered, do not trap positrons and hence do not modify the calculated annihilation signals. However, when positrons are already confined in one dimension to the interface regions, the removal of N atoms from the interface modifies the positron annihilation signals to an observable extent. Comparison of the theoretical predictions and the experimental data in Fig. 5(c) gives strong support for positron trapping at open-volume features involving V_N (but not V_{Ga}) localized at the (Al, Ga)N/GaN interface. A high concentration of V_N leads to such changes in ratio curves as the increased S parameter and lower intensity at high momenta. If the V_N are in the neutral charge state, as is likely in n-type material [10,11], they will not modify the electric fields driving positron (or hole) confinement at the interface.

Nitrogen vacancies act as deep donors in both GaN and AlN [10,11], and can hence act as hole traps in these materials, and likely also in (Al, Ga)N alloys. Our results on N-polar GaN/(Al, Ga)N/GaN heterostructures show that there is significant N deficiency at the bottom (Al, Ga)N/GaN interface, and that positrons are strongly attracted to this interface due to built-in electric fields when these are not screened by Si (n-type) doping in the (Al, Ga)N barrier. The nitrogen vacancies are likely to be in the neutral charge state at the interface, as a positive charge would prevent the positron confinement. Importantly, significant excess positive charge caused by, e.g., ionized donors at the bottom interface would also modify the built-in electric fields in such a way as to prevent positron confinement at the interface. Taking into account the width of the quasi-two-dimensional positron state [13], roughly 1/30 of the N atoms in the interface region need to be removed for a noticeable effect in the positron annihilation signal in the calculations. This suggests that the V_N sheet concentration is of the order of 10^{14} cm^{-2} in the experiments, comparable to the sheet-carrier concentration at the top interface of HEMTs [5]. Positron localization at the bottom (Al, Ga)N/GaN interface due to the electric fields implies a scenario where excess holes are driven to that interface and get trapped at the abundant N vacancies, causing the current collapse during operation observed in Ref. [3] for unoptimized N-polar HEMTs with $Al_{0.3}Ga_{0.7}N$ layer, and explains the improvement of the device properties with Si doping of the (Al, Ga)N barrier [3,8]. Interestingly, similar trap states are observed at the complementary net-negative-polarization interface of Ga-polar GaN/InGaN/GaN heterostructures [38]. Also, N deficiency at the InN/GaN and InGaN/GaN growth interface (In/Ga polarity, net negative polarization) has been reported, observed through the increase in the number of V_N in $V_{In} - nV_N$ complexes dominating the positron annihilation signals [39–43]. We suggest that N vacancies can be a universal detrimental donorlike interface trap in nitride semiconductor structures.

IV. SUMMARY

We show that N-polar GaN/(Al, Ga)N/GaN heterostructures exhibit significant N deficiency at the bottom (Al, Ga)N/GaN interface, and that these N vacancies can hamper the device performance through trapping of holes in unoptimized HEMT device structures. We arrive at this conclusion by performing positron annihilation experiments on HEMT-like structures, as well as state-of-the-art theoretical calculations of the positron states and positron-electron annihilation signals. We observe strong positron confinement at the bottom interface where the annihilation signal indicates the presence of a high concentration of N vacancies, but only in heterostructures where the built-in electric fields are not screened by, e.g., n-type doping of the (Al, Ga)N barrier. These built-in electric fields act upon free-carrier holes in the same way as for free positrons in the lattice, and N vacancies likely act as efficient hole traps due to their deep-donor character. We suggest the abundance of interfacial N vacancies with detrimental donorlike character to be a universal feature in nitride semiconductor heterostructures at net-negative-polarization interfaces.

ACKNOWLEDGMENTS

We acknowledge the computational resources provided by the Aalto Science-IT project and CSC—Finnish IT Centre for Science. This work is partially supported by the Academy of Finland Grants No. 285809, No. 315082, and No. 319178. The work at UCSB is supported by the Office of Naval Research (Dr. Paul Maki).

[1] D. Nirmal and J. Ajayan*Handbook for III-V High Electron Mobility Transistor Technologies* (CRC Press, Boca Raton, 2019).

[2] F. Bernardini and V. Fiorentini, Macroscopic polarization and band offsets at nitride heterojunctions, Phys. Rev. B **57**, R9427 (1998).

[3] S. Rajan, A. Chini, M. H. Wong, J. S. Speck, and U. K. Mishra, N-polar GaN/AlGaN/GaN high electron mobility transistors, J. Appl. Phys. **102**, 044501 (2007).

[4] L. Bjaalie, B. Himmetoglu, L. Weston, A. Janotti, and C. G. Van de Walle, Oxide interfaces for novel electronic applications, New J. Phys. **16**, 025005 (2014).

[5] B. Romanczyk, S. Wienecke, M. Guidry, H. Li, E. Ahmadi, X. Zheng, S. Keller, and U. K. Mishra, Demonstration of constant 8 W/mm power density at 10, 30, and 94 GHz in state-of-the-art millimeter-wave N-polar GaN MISHEMTs, IEEE Trans. Electron. Devices **65**, 45 (2018).

[6] P. S. Park and S. Rajan, Simulation of short-channel effects in N- and Ga-polar AlGaN/GaN HEMTs, IEEE Trans. Electron. Devices **58**, 704 (2011).

[7] K. Prasertsuk, T. Tanikawa, T. Kimura, S. Kuboya, T. Suemitsu, and T. Matsuoka, N-polar GaN/AlGaN/GaN metal-insulator-semiconductor high-electron-mobility transistor formed on sapphire substrate with minimal step bunching, Appl. Phys. Express **11**, 015503 (2018).

[8] M. H. Wong, S. Keller, S. D. Nidhi, D. J. Denninghoff, S. Kolluri, D. F. Brown, J. Lu, N. A. Fichtenbaum, E. Ahmadi, U. Singisetti, A. Chini, S. Rajan, S. P. Denbaars, J. S. Speck, and U. K. Mishra, N-polar GaN epitaxy and high electron mobility transistors, Semicond. Sci. Technol. **28**, 074009 (2013).

[9] B. Ozden, M. P. Khanal, S. Youn, V. Mirkhani, K. Yapabandara, M. Park, M. Zhao, H. Liang, P. K. Kandaswamy, and Y. N. Saripalli, Analysis of point defect distributions in AlGaN/GaN heterostructures via spectroscopic photo current-voltage measurements, ECS J. Solid State Sci. Technol. **5**, P3206 (2016).

[10] Q. Yan, A. Janotti, M. Scheffler, and C. G. Van de Walle, Origins of optical absorption and emission lines in AlN, Appl. Phys. Lett. **105**, 111104 (2014).

[11] J. L. Lyons and C. G. Van de Walle, Computationally predicted energies and properties of defects in GaN, npj Comput. Mater. **3**, 12 (2017).

[12] F. Tuomisto and I. Makkonen, Defect identification in semiconductors with positron annihilation: Experiment and theory, Rev. Mod. Phys. **85**, 1583 (2013).

[13] I. Makkonen, A. Snicker, M. J. Puska, J.-M. Mäki, and F. Tuomisto, Positrons as interface-sensitive probes of polar semiconductor heterostructures, Phys. Rev. B **82**, 041307 (2010).

[14] S. Keller, N. A. Fichtenbaum, F. Wu, D. Brown, A. Rosales, S. P. DenBaars, J. S. Speck, and U. K. Mishra, Influence of the substrate misorientation on the properties of N-polar GaN films grown by metal organic chemical vapor deposition, J. Appl. Phys. **102**, 083546 (2007).

[15] S. Keller, C. S. Suh, Z. Chen, R. Chu, S. Rajan, N. A. Fichtenbaum, M. Furukawa, S. P. DenBaars, J. S. Speck, and U. K. Mishra, Properties of N-polar AlGaN/GaN heterostructures and field effect transistors grown by metalorganic chemical vapor deposition, J. Appl. Phys. **103**, 033708 (2008).

[16] S. Keller, G. Parish, P. T. Fini, S. Heikman, C.-H. Chen, N. Zhang, S. P. DenBaars, and U. K. Mishra, Metalorganic chemical vapor deposition of high mobility AlGaN/GaN heterostructures, J. Appl. Phys. **86**, 5850 (1999).

[17] P. E. Blöchl, Projector augmented-wave method, Phys. Rev. B **50**, 17953 (1994).

[18] G. Kresse and J. Furthmüller, Efficient iterative schemes for ab initio total-energy calculations using a plane-wave basis set, Phys. Rev. B **54**, 11169 (1996).

[19] G. Kresse and J. Furthmüller, Efficiency of ab-initio total energy calculations for metals and semiconductors using a plane-wave basis set, Comput. Mater. Sci. **6**, 15 (1996).

[20] G. Kresse and D. Joubert, From ultrasoft pseudopotentials to the projector augmented-wave method, Phys. Rev. B **59**, 1758 (1999).

[21] E. Boroński and R. M. Nieminen, Electron-positron density-functional theory, Phys. Rev. B **34**, 3820 (1986).

[22] M. Alatalo, B. Barbiellini, M. Hakala, H. Kauppinen, T. Korhonen, M. J. Puska, K. Saarinen, P. Hautojärvi, and R. M. Nieminen, Theoretical and experimental study of positron annihilation with core electrons in solids, Phys. Rev. B **54**, 2397 (1996).

[23] I. Makkonen, M. Hakala, and M. J. Puska, Modeling the momentum distributions of annihilating electron-positron pairs in solids, Phys. Rev. B **73**, 035103 (2006).

[24] I. Makkonen, M. Hakala, and M. J. Puska, Calculation of valence electron momentum densities using the projector augmented-wave method, J. Phys. Chem. Solids **66**, 1128 (2005).

[25] J. Oila, V. Ranki, J. Kivioja, K. Saarinen, P. Hautojärvi, J. Likonen, J. M. Baranowski, K. Pakula, T. Suski, M. Leszczynski, and I. Grzegory, Influence of dopants and substrate material on the formation of Ga vacancies in epitaxial GaN layers, Phys. Rev. B **63**, 045205 (2001).

[26] A. Zubiaga, J. A. Garcia, F. Plazaola, F. Tuomisto, J. Zuniga-Perez, and V. Munoz-Sanjose, Positron annihilation spectroscopy for the determination of thickness and defect profile in thin semiconductor layers, Phys. Rev. B **75**, 205305 (2007).

[27] F. Tuomisto, T. Paskova, S. Figge, D. Hommel, and B. Monemar, Vacancy defect distribution in heteroepitaxial a-plane GaN grown by hydride vapor phase epitaxy, J. Cryst. Growth **300**, 251 (2007).

[28] F. Tuomisto, T. Paskova, R. Kröger, S. Figge, D. Hommel, B. Monemar, and R. Kersting, Defect distribution in a-plane GaN on Al_2O_3, Appl. Phys. Lett. **90**, 121915 (2007).

[29] A. Uedono, T. Fujishima, D. Piedra, N. Yoshihara, S. Ishibashi, M. Sumiya, O. Laboutin, W. Johnson, and Tomás Palacios, Annealing behaviors of vacancy-type defects near interfaces between metal contacts and GaN probed using a monoenergetic positron beam, Appl. Phys. Lett. **105**, 052108 (2014).

[30] A. Uedono, M. Malinverni, D. Martin, H. Okumura, S. Ishibashi, and N. Grandjean, Vacancy-type defects in Mg-doped GaN grown by ammonia-based molecular beam epitaxy probed using a monoenergetic positron beam, J. Appl. Phys. **119**, 245702 (2016).

[31] A. van Veen, H. Schut, J. de Vries, R. A. Hakvoort, and M. R. Ijpma, Analysis of positron profiling data by means of "VEPFIT", AIP Conf. Proc. 218, 171 (1991).

[32] A. Uedono, K. Tenjinbayashi, T. Tsutsui, Y. Shimahara, H. Miyake, K. Hiramatsu, N. Oshima, R. Suzuki, and S. Ishibashi, Native cation vacancies in Si-doped AlGaN studied by monoenergetic positron beams, J. Appl. Phys. **111**, 013512 (2012).

[33] S. F. Chichibu, A. Uedono, K. Kojima, H. Ikeda, K. Fujito, S. Takashima, M. Edo, K. Ueno, and S. Ishibashi, The origins and properties of intrinsic nonradiative recombination centers in wide bandgap GaN and AlGaN, J. Appl. Phys. **123**, 161413 (2018).

[34] M. A. Reshchikov, A. Usikov, H. Helava, Yu. Makarov, V. Prozheeva, I. Makkonen, F. Tuomisto, J. H. Leach, and K. Udwary, Evaluation of the concentration of point defects in GaN, Sci. Rep. **7**, 9297 (2017).

[35] J. Slotte, F. Tuomisto, K. Saarinen, C. G. Moe, S. Keller, and S. P. DenBaars, Influence of silicon doping on vacancies and optical properties of $Al_xGa_{1-x}N$ thin films, Appl. Phys. Lett. **90**, 151908 (2007).

[36] S. Hautakangas, I. Makkonen, V. Ranki, M. J. Puska, K. Saarinen, X. Xu, and D. C. Look, Direct evidence of impurity decoration of Ga vacancies in GaN from positron annihilation spectroscopy, Phys. Rev. B **73**, 193301 (2006).

[37] F. Tuomisto, V. Prozheeva, I. Makkonen, T. H. Myers, M. Bockowski, and H. Teisseyre, Amphoteric Be in GaN: Experimental Evidence for Switching between Substitutional and Interstitial Lattice Sites, Phys. Rev. Lett. **119**, 196404 (2017).

[38] C. A. Schaake, D. F. Brown, B. L. Swenson, S. Keller, J. S. Speck, and U. K. Mishra, A donor-like trap at the InGaN/GaN interface with net negative polarization and its possible consequence on internal quantum efficiency, Semicond. Sci. Technol. **28**, 105021 (2013).

[39] C. Rauch, I. Makkonen, and F. Tuomisto, Identifying vacancy complexes in compound semiconductors with positron annihilation spectroscopy: A case study of InN, Phys. Rev. B **84**, 125201 (2011).

[40] C. Rauch, F. Tuomisto, A. Vilalta-Clemente, B. Lacroix, P. Ruterana, S. Kraeusel, B. Hourahine, and W. J. Schaff, Defect evolution and interplay in n-type InN, Appl. Phys. Lett. **100**, 091907 (2012).

[41] C. Rauch, Ö. Tuna, C. Giesen, M. Heuken, and F. Tuomisto, Point defect evolution in low-temperature MOCVD growth of InN, Phys. Status Solidi A **209**, 87 (2012).

[42] A. Uedono, T. Watanabe, S. Kimura, Y. Zhang, M. Lozac'h, L. Sang, S. Ishibashi, N. Oshima, R. Suzuki, and M. Sumiya, Vacancy-type defects in $In_xGa_{1-x}N$ grown on GaN templates probed using monoenergetic positron beams, J. Appl. Phys. **114**, 184504 (2013).

[43] V. Prozheeva, I. Makkonen, R. Cusco, L. Artus, A. Dadgar, F. Plazaola, and F. Tuomisto, Radiation-induced alloy rearrangement in $In_xGa_{1-x}N$, Appl. Phys. Lett. **110**, 132104 (2017).